On the Influence of Dielectric Loss in Piezoelectric Energy Harvesting with SSHI Interface

Junrui Liang and Wei-Hsin Liao*

Smart Materials and Structures Laboratory, Department of Mechanical and Automation Engineering, The Chinese University of Hong Kong, Shatin, N. T., Hong Kong, China

ABSTRACT

Piezoelectric energy harvesting (PEH) is one of the promising techniques that can be utilized to scavenge energy from ambient mechanical vibration sources. The harvesting efficiency can be greatly improved with the switching interface called synchronized switch harvesting on inductor (SSHI). Most theoretical models were proposed with the emphasis on its ability to enhance harvesting efficiency. However, we found from experiments that, the voltage across the piezoelectric element reverses a little bit after every inversion, so as to weaken the inversion effect produced by the switching LCR shortcut. This reversion, although small compared to the inversion, decreases the voltage magnitude a lot, therefore diminishes the harvesting efficiency. In previous studies, the analytical results, which use the measured effective inversion factor in calculation, agreed with experiments; yet, the origin of the reversion after every switching action, as well as the quantitative relation between the ideal and effective inversion factors are also of interest. After experimentally investigating the SSHI circuit, we found that the reason of the reversion after every inversion is attributed to the influence of dielectric loss within the piezoelectric element. In this paper, a revised model considering this influence is introduced. With this model, not only the reason, which causes the reversion after every inversion, can be explained; but also the quantitative relation between the ideal and effective inversion factors can be obtained. Experiments are also conducted to validate the revised model.

Keywords: piezoelectric, energy harvesting, dielectric loss, SSHI

INTRODUCTION

Ubiquitous deployed sensor networks and mobile electronics are most potential applications which might gain benefit from the development on the techniques of *energy harvesting* (also known as *power harvesting* and *energy scavenging*) [1, 2]. In these fields, until now, most of the devices are powered by batteries. Due to batteries' capability in energy storage, these devices inevitably face the problems on limited lifetime and bothering replacement or recharging for batteries. On the other hand, instead of installing batteries to store enough energy to power these autonomous devices over a long working period, energy might be continually obtained from ambient sources (e.g., solar power,

^{*} Corresponding author: Tel: (852) 2609 8341; Fax: (852) 2603 6002; E-mail: whliao@cuhk.edu.hk

thermal energy, wind energy, and vibration energy) by equipping small energy harvesters.

Piezoelectric energy harvesting (PEH) is one of the promising techniques that can scavenge energy from ambient vibration sources. With its electromechanical coupling characteristic, a piezoelectric element can generate electricity when strain is produced. Since the deformation in vibrating structures is alternating, the generated electricity is also alternating. An interface circuitry is needed for AC-DC conversion. The standard energy harvesting (SEH) interface involves only a bridge rectifier for the AC-DC conversion [3]. To further improve the energy harvesting efficiency, Guyomar et al. proposed a treatment named *synchronized switching harvesting on inductor* (SSHI) [4]. It was claimed that, under the same displacement excitation, SSHI can increase the harvested power by several hundred percents, compared to SEH [4, 5].

The inversion factor γ plays an important role in the SSHI treatment. Theoretically, the harvesting power can reach infinity when γ approaches -1 [5]. In addition, the effective inversion was regarded to be only related to the quality factor of the inductive shortcut. Yet, in experiment, since a voltage reversion is found right after every voltage inversion across the piezoelectric element. The effective inversion factor in fact is always larger than the theoretical one, so that the inversion effect is weakened. It makes the practical voltage magnitude, as well as the harvesting power, much smaller than those in theoretical prediction with ideal inversion factor. Most literatures on SSHI only emphasized its outstanding capability on enhancing the harvesting efficiency; the effective inversion factor used in calculation was obtained from measurement. This phenomenon on reversion and the difference between the ideal and effective inversion factors are ignored previously.

Given a SSHI system constructed with ideal piezoelectric element and switching path, this phenomenon cannot be explained. After investigating the practical SSHI circuit, we found that the reversion is attributed to the *dielectric loss*, which induces internal leakage within the piezoelectric element. Besides the piezoelectric capacitance, the dielectric loss is another important electrical characteristic of piezoelectric materials in practical energy harvesting systems. But it was seldom considered in the PEH researches. Early studies on piezoelectric ceramics have already shown that the dielectric loss increases remarkably under high-power operation [6]. Therefore, as SSHI boosts the voltage across the piezoelectric element, which increases the transduction power, the dielectric loss is not of little influence to a PEH system. The purpose of this paper is to provide a detailed description on the phenomenon of voltage reversion after every inversion, as well as propose a revised model to analyze the influence of dielectric loss in PEH with SSHI interface.

PIEZOELECTRIC ENERGY HARVESTING WITH SSHI INTERFACE

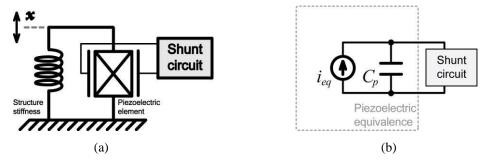


Figure 1. Schematic representation and commonly used equivalent circuit of a typical piezoelectric device. (a) Schematic representation. (b) Commonly used equivalent circuit.

Given a typical piezoelectric device, e.g., a piezoelectric cantilever with shunt circuit, its single degree of freedom (SDOF) schematic representation is shown in Figure 1(a). Under harmonic displacement excitation, the piezoelectric element was commonly modeled as an equivalent current source i_{eq} in parallel with the piezoelectric clamped capacitance C_p , as shown in Figure 1(b). i_{eq} is proportional to the velocity \dot{x} with the relation of

$$i_{eq}(t) = \alpha_e \ \dot{x}(t) \tag{1}$$

where α_e is the piezoelectric force-voltage coupling factor.

Different shunt circuits for different treatments are designed to extract energy from the vibrating mechanical structure. For the purpose of structural damping, the extracted energy is directly dissipated; while for energy harvesting, a portion of the extracted energy is reclaimed and stored in electrical form for subsequent usage.

In a vibrating piezoelectric element, since the induced voltage across the piezoelectric capacitance is alternating, the most conventional way to turn an AC voltage into DC is to use a bridge rectifier for rectification and then a capacitor for filtering. The combination of bridge rectifier and filter capacitor forms the standard interface circuit that can be used for energy harvesting, i.e., SEH. Ottman et al. discussed the optimization to the SEH technique [3]. Yet, using SEH cannot ensure the energy is always flowing from mechanical part to electrical part. During a certain interval in every cycle, energy returns from electrical part to mechanical part. It was called *energy return phenomenon* [7].

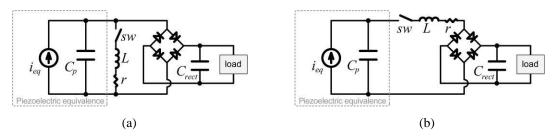


Figure 2. Equivalent circuits of two SSHI treatments. (a) p-SSHI. (b) s-SSHI.

The SSHI treatment overcomes this problem by adding an inductive switching path to the SEH circuit. This path can be connected in parallel to the bridge rectifier to form a p-SSHI circuit (Figure 2(a)), or in series to form an s-SSHI circuit (Figure 2(b)) [5]. Regardless of p-SSHI or s-SSHI, the inductive switching path switches on to form a series LCR loop once the displacement *x* reaches its extreme values¹, and then switches off after half of a LCR cycle, i.e.,

$$\tau = \pi \sqrt{LC} \tag{2}$$

The voltage across the capacitance, denoted as v_p , inverts during the short interval τ , which is much smaller than the mechanical cycle, with the ideal inversion factor of ²

$$\gamma = -e^{-\pi/(2Q)} \tag{3}$$

where Q is the quality factor of the LCR loop. Typical waveforms of p-SSHI or s-SSHI as well as the

¹ At these very instants, the velocity \dot{x} as well as the current i_{eq} cross zeros.

² This definition on voltage inversion factor differs from that given in [8]. The sign information is also included here.

zoom-in view to one of the switching processes are shown in Figure 3(a) ~ (c), respectively. Since i_{eq} is proportional to \dot{x} , these switching actions make v_p in phase with i_{eq} . It ensures that the power input from mechanical part to electrical part, which equals to the product of v_p and i_{eq} , is always positive. Moreover, the SSHI also boosts the magnitude of v_p to enable a larger power conversion.

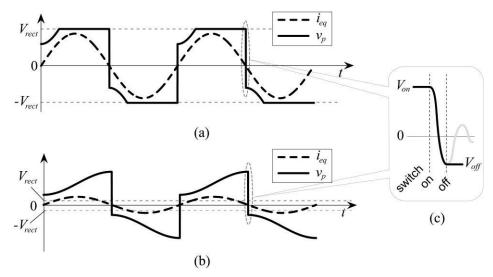


Figure 3. Typical waveforms of two SSHI treatments. (a) p-SSHI. (b) s-SSHI. (c) Inversion of v_p at the instant of extreme displacements.

INFLUENCE OF DIELECTRIC LOSS

SSHI does provide an effective mechanism to increase the harvesting energy under same excitation level; the analytical results provided in the previous literatures match experiments as well. However, a phenomenon observed from the experimental waveform, which differs from that in ideal one, was ignored. In this section, with the focus on the s-SSHI interface, this phenomenon will be described and analyzed in detail.

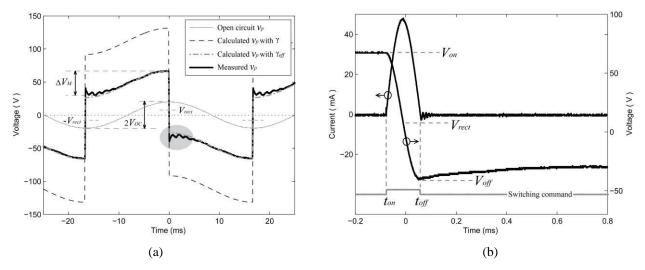


Figure 4. Characteristic waveforms in s-SSHI ($V_{OC} = 20$ volt, $V_{rect} = 7.6$ volt). (a) Voltages. (b) Zoom-in view to the voltage and current around time origin.

Phenomenon

Applying a 30 Hz constant (in magnitude) displacement excitation to a piezoelectric cantilever, whose first vibration resonant frequency is nearby, a 20 volt open circuit voltage is recorded across the piezoelectric element, i.e., $V_{OC} = 20$ volt. Figure 4(a) shows the voltage waveforms when s-SSHI treatment is activated under 7.6 volt rectified voltages³, i.e., $V_{rect} = 7.6$ volt. Figure 4(b) shows the zoom-in view to one of the switching instants around time origin. When the switching command is applied, the voltage level before and after the switching action can be obtained as V_{on} and V_{off} , as indicated in Figure 4(b). Substituting the measured V_{on} , V_{off} , and V_{rect} into the equation of

$$V_{off} - V_{rect} = \gamma \left(V_{on} - V_{rect} \right) \tag{4}$$

yields the ideal inversion factor of the LCR shortcut $\gamma = -0.8$. Ideally, without any loss, the effect of SSHI treatment is to, intuitively, split the open circuit voltages at maxima places and move the adjacent parts against each other to some extent. Lefeuvre et al. gave the formulas with which the s-SSHI characteristic voltage waveform can be theoretically obtained [5]. Based on these formulas, the dash curve in Figure 4(a) shows the theoretical waveform of v_p with $\gamma = -0.8$. Nevertheless, there is a large error between the calculated result and the experimental one (bold curve). Two features, which differ from those in theoretical waveform, can be observed from the experimental waveform:

- 1. As highlighted by the ellipse area in Figure 4(a), the voltage v_p reverses somewhat right after every inversion. Small damped oscillation can be observed as well.
- 2. The measured voltage difference between two switching instants in s-SSHI, i.e., ΔV_M , as indicated in Figure 4(a), is smaller than, rather than equals to, that in open circuit condition, i.e., $2V_{OC}$.

For the first feature, similarities can be observed from the experimental waveforms provided in [8-10]. This reversion counteracts the inversion, therefore makes the effective inversion factor above the ideal inversion factor γ , implying that the inversion effect is weakened. A small decrease in inversion factor usually causes large drop in the magnitude of v_p . The second feature imposes an equivalent effect as to decrease V_{OC} , which also results in the magnitude degradation of v_p . These two features were not pointed out in the previous literatures, not to mention the origin of them. However, their theoretical results still agreed with the experiments, because, instead of using the ideal inversion factor γ in calculation, they used the effective inversion factor (denoted as γ_{eff} in the following part of this paper), which can be estimated by taking V_{off} as the voltage level after the reversion. But still, the reason about the voltage reversion, as well as the relation between γ and γ_{eff} is of interest.

These questions can be studied with an investigation to the voltage and current in one of the switching instants. As far as v_p is proportional to the charge stored in the piezoelectric capacitance C_p , the reversion of v_p after every inversion must be resulted from some current leakage. For the observation of the instant current flowing through the treatment circuit during the switching instant, a 10Ω current sampling resistor is connected to the treatment circuit in series. As shown in Figure 4(b), the switch begins to conduct at t_{on} , and then is blocked again at t_{off} . The current approaches zero quickly after the switching path is blocked again at t_{off} , in spite of some low level oscillation. However, v_p keeps reversing even no current leaks through the shunt circuit⁴. Therefore, the current leakage should

³ The effective rectified voltage V_{rect} is the sum of V_{store} the voltage across C_{rect} , and V_F , the forward voltage gap of the bridge rectifier. V_{store} is regarded as constant during every vibration cycle, since C_{rect} is usually selected much larger than C_p . V_F is about 1.0 volt in our experimental circuit.

⁴ As far as oscilloscope probe with high input impedance is used in experiments, it is considered that little current leaks through the measurement process as well.

take place internally within the piezoelectric element.

In essence, the voltage reversion in SSHI is caused by the dielectric loss within the piezoelectric element, which was not mentioned in the previous studies on PEH with SSHI.

On the other hand, in the studies for piezoelectric ceramics, it was reported that the influence of dielectric loss increases intensively under high-power operation [6]. As far as SSHI treatment boosts the voltage level across the piezoelectric element, as well as the conversion power, it is rational that the dielectric loss influences the harvesting system more, when conversion power is getting larger. The conventional model, as given in Figure 1(b), which considered the piezoelectric element as a lossless component, is no longer capable to show details on the mechanism of voltage reversion in SSHI.

Revised equivalent circuit

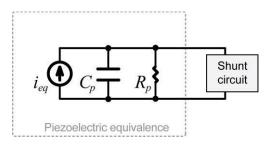


Figure 5. Revised equivalent circuit of a piezoelectric device.

The high-power characteristics of piezoelectric transducers can be studied with a more comprehensive model [11], based on which the internal losses can also be taken into account. In order to evaluate on the influence of dielectric loss in PEH system with SSHI interface, Figure 5 shows the revised equivalent circuit of a piezoelectric device. An equivalent parallel resistance (EPR) R_p is internally connected to the current source and the piezoelectric capacitance. The shunt circuit can be connected as either p-SSHI or s-SSHI. During the harvesting process, the charge stored in C_p might leak internally through this EPR path, resulting in the voltage reversion and further magnitude degradation of v_p in SSHI.

Effective inversion factor

In s-SSHI treatment, besides (4), another relation links the voltages at the start (V_{off}) and end (V_{on}) of a switch-off interval. Mark one of the switching on maximum actions as time origin. The voltage v_p in the following half cycle is

$$v_p(t) = V_{off} + \frac{1}{C_p} \int_0^t \left[i_{eq}(t) - \frac{v_p(t)}{R_p} \right] dt$$
(5)

As far as

$$v_p(T/2) = -V_{on} \tag{6}$$

where T is the period of mechanical excitation, and

$$\frac{1}{C_p} \int_0^{T/2} i_{eq}(t) \, \mathrm{d}t = -2V_{OC} \tag{7}$$

substituting (6) and (7) into (5) at t = T/2 instant, we can have

$$-V_{on} = V_{off} - 2V_{OC} - \frac{1}{R_{p}C_{p}} \int_{0}^{T/2} v_{p}(t) dt$$
 (8)

(8) can be further simplified by estimating $v_p(t)$ with its first-order approximation in this 0 to T/2 interval

$$\widetilde{v}_{p}(t) = V_{off} - \frac{2(V_{on} + V_{off})}{T}t, \qquad t \in [0, T/2]$$

$$\tag{9}$$

Substituting this approximated v_p into (8) yields

$$-V_{on} = V_{off} - 2V_{OC} - \frac{T}{4R_{p}C_{p}} \left(V_{off} - V_{on}\right)$$
 (10)

where V_{OC} , the open circuit voltage can be directly measured without the SSHI circuit connected. With the two linear equations of (4) and (10), the values of V_{on} and V_{off} can be solved out.

In addition, at low excitation level, the difference between ΔV_M and $2V_{OC}$ is not significant, i.e., the effect produced by the second observed feature can be neglected, compared to that by first one. Considering the cancellation of reversion towards inversion, the pseudo V_{off} , i.e., voltage value after the reversion, is

$$V_{off, ps} = 2V_{OC} - V_{on} \tag{11}$$

This $V_{off, ps}$ is usually measured from experimental waveforms and taken as effective V_{off} in the previous studies. Furthermore, from (4) and (10), the effective inversion factor γ_{eff} is defined as

$$\gamma_{eff} = \frac{V_{off, ps} - V_{rect}}{V_{on} - V_{rect}} = \gamma + \frac{T}{4R_p C_p} (1 - \gamma)$$
(12)

Since γ is less than one, therefore γ_{eff} is greater than γ . In general, the inversion effect is weakened. In Figure 4(a), it shows that, with γ_{eff} , the calculated waveform (dash dot curve) approaches the experimental one quite well⁵. From (3), γ approaches -1 when the quality factor of the LCR path, i.e. Q, approaches infinity. Substituting this limitation on γ to (12), we can obtain the limitation of the effective inversion factor as

$$\lim_{\gamma \to -1} \gamma_{eff} = \frac{T}{2R_n C_n} - 1 \tag{13}$$

-

⁵ Detailed parameters of the experimental system are provided in "Experiments" section.

Obviously, the effective inversion factor γ_{eff} and also its limitation are not only determined by the quality factor of the switching LCR path, but also depend on the dielectric loss of the selected piezoelectric element, as well as the vibration period.

Energy flow

As pointed out by Liang and Liao in [7], energy harvesting is not the only function generated within the PEH system; during the harvesting process, another portion of energy may be dissipated in the conditioning circuits of the treatment. In addition, both energy harvesting and dissipation extract energy from the vibrating structure, and consequently bring out structural damping. Therefore, in order to have comprehensive evaluation to a certain PEH system, not only the harvesting capability, but also the side effect on energy dissipation should be taken into consideration.

With the analysis above, in an s-SSHI system, the amount of energy harvested in one cycle is

$$E_h = 2V_{store}C_p(V_{on} - V_{off})$$
(14)

The amount of energy dissipated in one cycle is

$$E_{d} = C_{p} (V_{on} - V_{rect})^{2} (1 - \gamma^{2}) + 2V_{F} C_{p} (V_{on} - V_{off}) + 2 \int_{0}^{T/2} \frac{1}{R_{p}} \widetilde{v}_{p}(t)^{2} dt$$
 (15)

The three items in (15) are sequentially corresponding to: the dissipation induced by the equivalent series resistance (ESR) of the switching path, i.e., r in Figure 2; the dissipation induced by the bridge rectifier; and the dielectric loss induced by the EPR R_p ⁶.

EXPERIMENTS

Experiments are performed, in order to measure the ERP R_p in the revised equivalent circuit, and further validate our analysis with an emphasis on energy flow.

Figure 6 shows the experimental setup. The main mechanical structure is a base excited aluminium cantilever, whose excitation is from a shaker (Mini Shaker Type 4810, B & K). A piezoceramic patch of 49mm x 24mm x 0.508mm (T120-A4E-602, Piezo System, Inc.) is bonded near the fixed end where the largest strain happens along the cantilever. For the purpose of synchronization, an electromagnetic sensor is employed to sense the relative velocity between the cantilever end and the base. The permanent magnet acts as proof mass at the same time. It can lower the vibration frequency and increase the displacement of the free end. The output voltage from the coil, which is proportional to the end velocity, then is input to a micro-controller unit (eZ430-RF2500, Texas Instrument). In the circuitry part, the micro-controller is coded to firstly analyze the velocity signal, and then generate switching command to drive two MOSFET switches to perform synchronized switching actions. Although the micro-controller is powered by batteries, there are two advantages for this setup, compared to those which were commonly used in the previous studies [4, 5]. By adopting the electromagnetic velocity sensor, rather than inductive displacement sensor, self-powered sensing is achieved. Meanwhile, since the velocity signal is obtained directly, zero-crossing detection rather

⁶ For simplicity, the first-order approximation of $v_p(t)$ is also used to estimate the dissipated energy here.

than peak detection is required, which might help to save some computing effort. By equipping a micro-controller unit, which works independently and provides accesses to many peripheral devices, e.g., sensors, RF unit, and power management unit, we are getting closer towards the goal of constructing an intelligent autonomous device.

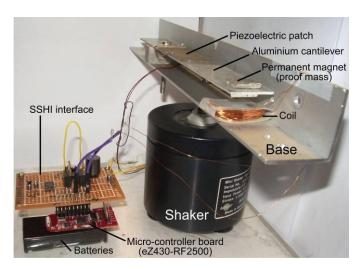


Figure 6. Experimental setup.

Table 1 gives some parameters of the experimental setup, including mechanical structure, interface circuitry as well as the excitation.

Table 1. Parameters of the experimental setup.

Parameter	f_{OC}	f_{SC}	f_0	C_p	C_{rect}	L	SW	Rectifier
Value	27.31 Hz	27.06 Hz	30.0 Hz	34.76 nF	10 μF	47 mH	MOSFET	DB104
							(IRL510)	$(V_F = 1.0V)$

Measuring the EPR R_p

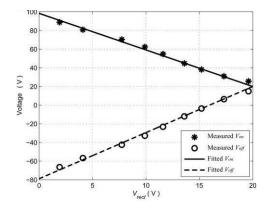


Figure 7. Fitting the experimental data of V_{on} and V_{off} to obtain the value of R_p .

The measurement on dielectric loss under high power operation is an issue. The loss is nonlinear, and it increases significantly under high power operation [6, 10]. In this paper, a linear resistance R_p is

used to approximately model the influence of dielectric loss. To determine the value of R_p , the voltages of V_{on} and V_{off} under different rectified voltage V_{rect} are measured first. As far as R_p is related to the theoretical V_{on} and V_{off} with (4) and (10), the value of R_p can be obtained simultaneously with the process of fitting the measured V_{on} and V_{off} data sets with the least square method.

The measured data as well as the fitted lines are shown in Figure 7. From the measured data, the ideal inversion factor $\gamma = -0.80$. From the curve fitting process, the corresponding $R_p = 2.07 \text{ M}\Omega$. Therefore, with (12), the effective inversion factor can be calculated $\gamma_{eff} = -0.59$.

Results

Experiments on both functions of energy harvesting and dissipation are performed in order to check their correlation to the revised theory, which includes the influence of dielectric loss. Load resistors with different values are connected as DC load. Recording the voltage V_{store} across the load, the harvesting power can be obtained with the Joule's laws. As for the energy dissipation, three parts should be measured individually. Power dissipated by the bridge rectifier is related to the harvesting. A sampling resistor is connected to the switching path to extract the RMS current flowing through the path, so as to estimate the power dissipation of its ESR r. The dissipation by R_p can be obtained with the RMS value of v_p .

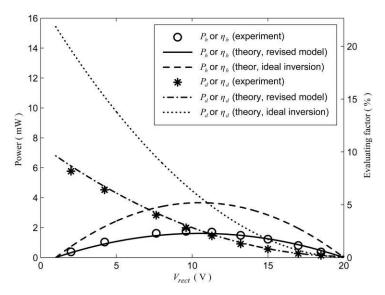


Figure 8. Power and evaluating factors in PEH with s-SSHI interface.

For theoretical result, as (14) and (15) give the harvested and dissipated energy in every vibration cycle, multiplying E_h and E_d with the vibration frequency f_0 yields the power on energy harvesting and dissipation, i.e., P_h and P_d , as shown in Figure 8. Meanwhile, besides the absolute power, the relative indices, i.e., efficiencies on energy harvesting and dissipation towards the energy associated with vibration are also of interest. These two indices were defined as harvesting factor η_h and dissipation factor η_d [7]. In this study, since constant displacement excitation is applied⁷, the energy associated with vibration, usually denoted as E_{max} , does not change. It can be derived with the coupling coefficient k_d^2 , which can be obtained with the natural frequencies under open and short circuit conditions,

⁷ The relative displacement between the cantilever and the base may change when the SSHI treatment is activated. In experiment, the shaker input is adjusted to maintain the same vibration level according to the sensed velocity.

i.e., f_{OC} and f_{SC} in Table 1. With the definition on η_h and η_d , they are proportional to P_h and P_d . The corresponding scale of the two evaluating factors is given by the right vertical axis in Figure 8.

Figure 8 shows that both experimental results and theoretical analyses agree with each other well. In addition, for comparison, the theoretical result with ideal inversion, i.e., assuming no reversion follows inversion, is also shown. Both predicted harvested power and dissipated power with this model are nearly 100% higher than those in real situation. Therefore, the reversion produced by dielectric loss, although small compared to the inversion, significantly degrades the efficiencies on energy harvesting and dissipation.

CONCLUSIONS

Based on the previous theoretical analyses on PEH with SSHI interface, it was considered that, by adopting a really low loss switching LCR path, the harvesting power can be pushed towards infinity (ideal case without considering the effect on structural damping). Yet, in this paper, we showed that the power harvested is also much related to the dielectric loss within the piezoelectric element. This loss causes the voltage reversion across the piezoelectric element after every inversion, weakens the inversion effect, and consequently degrades the voltage magnitude as well as the harvesting efficiency a lot. The phenomenon on voltage inversion was explained. A revised model was proposed to include the influence of dielectric loss in the analysis. With this model, the relation between ideal and effective inversion factor was obtained; limitation on the effective inversion factor was recognized. Theoretical result of this revised model showed good agreement with the experimental data. In addition, for overall evaluation of PEH systems, instead of merely focusing on the harvesting power, the energy flow including harvested and dissipated energy and also their corresponding evaluating factors were emphasized.

ACKNOWLEDGEMENTS

The work described in this paper was supported by the grant from Research Grants Council (Project No. CUHK4152/08E) of Hong Kong Special Administrative Region, China.

REFERENCES

- 1. J. A. Paradiso and T. Starner, "Energy scavenging for mobile and wireless electronics," *IEEE Pervasive Computing*, vol. 4, no. 1, pp. 18-27, 2005.
- 2. S. R. Anton and H. A. Sodano, "A review of power harvesting using piezoelectric materials (2003-2006)," *Smart Materials and Structures*, vol. 16, no. 3, pp. R1-R21, 2007.
- 3. G. Ottman, H. Hofmann, A. Bhatt, and G. Lesieutre, "Adaptive piezoelectric energy harvesting circuit for wireless remote power supply," *IEEE Transactions on Power Electronics*, vol. 17, no. 5, pp. 669-676, 2002.
- 4. D. Guyomar, A. Badel, E. Lefeuvre, and C. Richard. "Toward energy harvesting using active materials and conversion improvement by nonlinear processing," *IEEE Transactions on Ultrasonics, Ferroelectrics and Frequency Control*, vol. 52, no. 4, pp. 584-595, 2005.
- 5. E. Lefeuvre, A. Badel, C. Richard, L. Petit, and D. Guyomar, "A comparison between several

- vibration-powered piezoelectric generators for standalone systems," *Sensors and Actuators A: Physical*, vol. 126, no. 2, pp. 405-416, 2006.
- 6. S. Hirose, M. Aoyagi, and Y. Tomikawa, "Dielectric loss in a piezoelectric ceramic transducer under high-power operation; increase of dielectric loss and its influence on transducer efficiency," *Japanese Journal of Applied Physics*, vol. 32, pp. 2418-2421, 1993.
- 7. J. R. Liang and W. H. Liao, "Piezoelectric energy harvesting and dissipation on structural damping," *Journal of Intelligent Material Systems and Structures*, vol. 20, no. 5, pp. 515-527, 2009.
- 8. M. Lallart and D. Guyomar, "An optimized self-powered switching circuit for non-linear energy harvesting with low voltage output," *Smart Materials and Structures*, vol. 17, pp. 1-8, 2008.
- 9. D. Guyomar, K. Yuse, T. Monnier, L. Petit, E. Lefeuvre, and C. Richard, "Semi-passive vibration control: principle and application," *Annals of the University of Craiova, Electrical Engineering series*, no. 30, pp. 57-62, 2006.
- 10. C. Richard, D. Guyomar, D. Audigier, and H. Bassaler, "Enhanced semi-passive damping using continuous switching of a piezoelectric device on an inductor," *Smart Structures and Materials* 2000: Damping and Isolation, SPIE, vol. 3989, pp. 288-299, 2000.
- 11. M. Umeda, K. Nakamura, and S. Ueha, "The measurement of high-power characteristics for a piezoelectric transducer based on the electrical transient response," *Japanese Journal of Applied Physics*, vol. 37, pp. 5322-5325, 1998.